Evidence of Multi-Process Matrix Diffusion in a Single Fracture from a Field Tracer Test

Quanlin Zhou [1], Hui-Hai Liu [1], Gudmundur S. Bodvarsson [1], and Fred J. Molz [2]

[1]Earth Sciences Division, Lawrence Berkeley National Laboratory, One Cyclotron Road, Berkeley, CA 94720, USA

[2]Department of Environmental Engineering and Science, Clemson University, Clemson, SC 29634, USA

Abstract

Compared to values inferred from laboratory tests on matrix cores, many field tracer tests in fractured rock have shown enhanced matrix diffusion coefficient values (obtained using a single-process matrix-diffusion model with a homogeneous matrix diffusion coefficient). To investigate this phenomenon, a conceptual model of multi-process matrix diffusion in a single-fracture system was developed. In this model, three matrix diffusion processes of different diffusion rates were assumed to coexist: (1) diffusion into stagnant water and infilling materials within fractures, (2) diffusion into a degraded matrix zone, and (3) further diffusion into an intact matrix zone. The validity of the conceptual model was then demonstrated by analyzing a unique tracer test conducted using a long-time constant-concentration injection. The tracer-test analysis was conducted using a numerical model capable of tracking the multiple matrix-diffusion processes. The analysis showed that in the degraded zone, a diffusion process with an enhanced diffusion rate controlled the steep rising limb and decay-like falling limb in the observed breakthrough curve, whereas in the intact matrix zone, a process involving a lower diffusion rate affected the long-term middle platform of slowly increasing tracer concentration. The different matrix-diffusion-coefficient values revealed from the field tracer test are consistent with the variability of matrix diffusion coefficient measured for rock cores with different degrees of fracture coating at the same site. By comparing to the matrix diffusion coefficient calibrated

using single-process matrix diffusion, we demonstrated that this multi-process matrix diffusion may contribute to the enhanced matrix-diffusion-coefficient values for single-fracture systems at the field scale.

Key words: matrix diffusion, fractured rock, tracer test, heterogeneity, groundwater, flow and transport

1. Introduction

Matrix diffusion is one of the key transport mechanisms in fractured media (e.g., Neretnieks, 2002; Zhou et al., 2003), and its importance has been confirmed by both single- and multi-tracer tests (e.g., Maloszewski et al., 1999). It has been found that the effective matrix diffusion coefficient (D_m^e) calibrated using field tracer tests can be orders of magnitude higher than the corresponding matrix diffusion coefficient (D_m) inferred from laboratory experiments on intact rock cores (Hodgkinson and Lever, 1983; Neretnieks, 2002; Andersson et al., 2004; Liu et al., 2004; Zhou et al., 2005). The enhanced matrix diffusion has been attributed to many different mechanisms, such as infilling materials and stagnant water within fractures (Neretnieks, 2002), a degraded and altered matrix zone adjacent to fractures (Hodgkinson and Lever, 1983; Maloszewski and Zuber, 1993; Andersson et al., 2004), and connected small fractures (Wu et al., 2004). The diffusion processes in these different media (as well as in the intact matrix rock) may co-exist for a given site, as evidenced by the computed tomography scanning of diffusion penetration into an artificially fractured chalk core (Polak et al., 2003) and laboratory diffusion experiments on fractured rock cores with different degrees of fracture coating (Skagius and Neretnieks, 1986). However, little evidence for the heterogeneous matrix diffusion in the field

has been obtained from field tracer tests, possibly because most of the tests (conducted using a pulse-injection technique) were not of long-enough duration to show all the processes, or because separating the processes from each other in a resulting breakthrough curve (BTC) was difficult.

Here, we propose a conceptual model of multi-process matrix diffusion to explain the enhancement of the effective matrix diffusion coefficient for single-fracture systems. To demonstrate the multi-process matrix diffusion in the field, we analyze a unique field tracer test (Gustafsson and Klockars, 1981; Davison et al., 1982; Hodgkinson and Lever, 1983). The test was conducted by constant-concentration injection over a long time. The BTC exhibited three distinct segments: (1) a steep rising limb, (2) a long middle platform with slow increase in concentration, and (3) a decay-like falling limb (see Figure 1). The numerical analysis based on the multi-process matrix diffusion model produces a good match between measured and calibrated BTCs, supporting the existence of multi-process matrix diffusion. For comparison, we also calibrate the test using the traditional single-process matrix diffusion model with a focus on short time responses (rising and falling limbs), and predict tracer transport behavior at different scales in a linear flow field.

2. Multi-Process Matrix Diffusion

Based on field surveys, laboratory observations, and field tracer test analyses, we developed a conceptual model of multi-process matrix diffusion for a single-fracture system. Matrix diffusion in a natural single-fracture system may exhibit three processes in a series: (1) diffusion into infilling materials and stagnant water within the fracture, (2) diffusion into a degraded and altered matrix zone adjacent to the fracture, and (3) further diffusion into an intact matrix zone. The three zones may have different matrix diffusion coefficient (D_m) values. The

diffusion coefficient for an isotropic matrix depends on matrix tortuosity, $\tau (>1)$, and the molecular diffusivity (D_w) of a solute in free water:

$$D_m = D_w/\tau . \quad (1)$$

Because the matrix tortuosity is a function of matrix porosity (ϕ_m) based on Archie's law (Boving and Grathwohl, 2001), we have

$$D_m = \phi_m^{n-1} D_w , \quad (2)$$

where n is an empirical parameter, which is generally larger than 2.0 for materials of low porosity.

The proposed multi-process matrix diffusion model is consistent with the different laboratory D_m and ϕ_m values in the three diffusion zones demonstrated by Skagius and Neretnieks (1986). They measured laboratory porosities and diffusion coefficients for a number of matrix cores sampled at different sites in Sweden. Some samples contained only intact matrix, while others contained crushed materials within fractures, fracture coating materials, or both. The average value of measured matrix porosity for the intact crystalline rock at the Finnsjon site was 0.3%, and the average D_m value was 2.67×10^{-11} m^2/s for iodide solution (Hodgkinson and Lever, 1983). For cores containing fracture-coating materials, the tests indicated that the degraded matrix zone had higher ϕ_m (4.9%) and D_m (6.1×10^{-11} m^2/s) values than those of intact matrix. For a crushed zone with surface fracture-coating materials, the measured matrix porosity was 7.5% and the average measured D_m value was 5.33×10^{-10} m^2/s, indicating that the crushed materials have matrix diffusion coefficients more than one order of magnitude larger than the intact matrix zone. Note that the above D_m values are calculated from the "effective"

matrix diffusion coefficient (D_e) values and matrix porosity from Skagius and Neretnieks (1986) and Hodgkinson and Lever (1983). D_e was defined as the product of the matrix diffusion coefficient (D_m) and matrix porosity (ϕ_m) for a conservative tracer. In addition, the laboratory tests also showed that matrix porosity decreases with penetration depth into the matrix, and the matrix diffusion coefficient has a similar trend. From this, we can assume that the presence of infilling materials within fractures and the degraded matrix zone enhances diffusive mass transfer between fractures and the matrix. Also note that the degraded zone here is similar to the "fracture surface zone" defined by Tokunaga and Wan (2001). Their laboratory measurements showed that porosity in the fracture surface zone is much higher than the value for the bulk matrix.

The multi-process matrix diffusion model is also consistent with field reports on infilling materials within fractures. The presence of fracture infilling materials has been revealed by field surveys (Wealthall et al., 2001) and infiltration tests on natural fractures in the unsaturated zone (Weisbrod et al., 2002). This conceptual model is also supported by a number of field tracer tests in single-fracture systems from which enhanced matrix diffusion coefficients have been calibrated, using the single-process matrix diffusion model with a homogeneous matrix diffusion coefficient (Neretnieks, 2002; Zhou et al., 2005). The calibrated values of matrix diffusion coefficient for these tests are orders of magnitude higher than laboratory values for the intact matrix zone. As demonstrated below, the calibrated values may be representative of diffusion processes occurring in the infilling materials within fractures and/or in the degraded matrix zone.

3. Evidence of Multi-Process Matrix Diffusion

3.1. Tracer Test

A unique tracer test was conducted for a fractured zone at the Finnsjon site, Sweden (Gustafsson and Klockars, 1981; Davison et al., 1982; Hodgkinson and Lever, 1983). Tracer (iodide) solution was injected into the fractured zone through a small (2 m thick) packed-off interval of an injection well, at a constant rate of 1.8×10^{-5} moles/s, for 350 hours. The tracer migrated to a pumping well located at a distance of $r_L = 30.0$ m from the injection well. The flow rate through the fractured zone was $Q = 2.0 \times 10^{-5}$ m^3/s. Continuous pumping and sampling was conducted for 600 hours. For the details of the tracer test, the readers should refer to Gustafsson and Klockars (1981) and Davison et al. (1982).

Figure 1 shows the BTC of iodide concentration observed at the pumping well. Three distinct stages can be observed: a steep rising limb, a relatively flat middle platform, and a decay-like falling limb. The tracer is captured in the pumping well at the 15th hour, after which its concentration increases steeply until the 40th hour. The rising limb represents a migrating solute front under dispersion and matrix diffusion. During the second stage, tracer concentration increases slowly as a main trend, with some fluctuations. The fluctuations at the early time (less than 100 hr) were caused by a couple of valve leakage detected during the test (Swedish Nuclear Power Inspectorate, 1986). During the third stage of the test, 12 days after the termination of tracer injection, tracer concentration starts to decrease, and then continues to decay.

This tracer test was selected to support the multi-process matrix diffusion model developed in Section 2, because it was unique in comparison with many field tracer tests, in the following ways. First, this test had a unique middle platform of the measured BTC with slowly increasing tracer concentrations, in comparison with pulse-injection tracer tests. This middle

platform exhibits the different signatures of the degraded matrix zone and the intact matrix zone caused by the long-time constant-concentration injection, indicating that the main trend in the middle platform is likely caused predominantly by matrix diffusion of multiple processes. Secondly, numerous laboratory rock-core data on the variability of matrix porosity and matrix diffusion coefficient with different degrees of fracture-coating materials are available to validate the calibrated transport parameters from the field tracer test (to be discussed in Sections 3.2 and 3.3).

The fractured zone may contain a number of individual fractures, depending on fracture frequency and spacing, which are not available for this site. As demonstrated by the vertical profiles of hydraulic conductivity along the injection and pumping wells, the hydraulic conductivity (4.35×10^{-6} m/s) of this fractured zone is relatively high (Gustafsson and Klockars, 1981). To simplify the following analyses, it is assumed, following Hodgkinson and Lever (1983), that the fracture zone considered here may be represented using a single fracture and its surrounding rock matrix.

3.2. Analytical Analysis (Calibration A)

To compare with the multi-process matrix diffusion model, this tracer test was first analyzed using a semi-analytical model (Reimus et al., 2003; Zhou et al., 2005), which tracks single-process matrix diffusion (a uniform matrix porosity and diffusion coefficient). The BTC observed in the tracer test was used to calibrate three transport parameters. The first parameter was the mean residence time of water, T_0, (defined as $T_0 = r_L/V$, where V is the mean fluid velocity). The second parameter was the Peclet number, P_e, (defined as $P_e = r_L/\alpha_L$, where α_L is the longitudinal dispersivity). The final parameter was the diffusive mass-transfer parameter,

A, (defined as $A = \frac{\phi_m}{b}\sqrt{D_m^e}$, where b is the half fracture aperture). In the calibration, we focused on the rising and falling limbs with a higher weight factor (for the misfit between calibrated and measured concentrations) than the middle platform, because the multi-process matrix diffusion cannot be fully captured by the semi-analytical model. The calibrated transport parameters were $T_0 = 20.95$ hr, $P_e = 50.5$, and $A = 0.108$ hr$^{-0.5}$.

As shown in Figure 1, an excellent match between the calibrated and measured rising limbs is obtained. The match between the calibrated and measured falling limbs is also very good. These matches indicate that the calibrated advection and dispersivity ($\alpha_L = 0.59$ m) are representative of the main flow path. Moreover, the calibrated A parameter accurately represents the matrix diffusion process for the rising and falling limbs. This process occurs in the degraded matrix zone within a short time after the beginning (for the rising limb) and termination (for the falling limb) of tracer injection.

The large value for the calibrated A parameter is, however, not suitable for the entire middle platform, as indicated by the poor match between calibrated and measured concentrations. The poor match may indicate that the later portion of the middle platform was controlled by a diffusion process different from that for the rising and falling limbs. To verify this concept, a smaller A value (corresponding to diffusion process in the intact matrix zone) was used with the calibrated T_0 and P_e values. As shown in Figure 1, the small A parameter produces a better match between simulated and measured concentrations for the later portion of the middle platform than the calibrated A value. However, this small A parameter value produces unacceptable matches for the rising and falling limbs. All these together indicate that *different*

diffusion processes dominated at different times, each decisively influencing a specific portion of the tracer BTC.

The multi-process matrix diffusion can also be interpreted by comparing a calculated matrix porosity value (based on the calibrated transport parameters) and the average measured value (0.3%) for intact matrix cores. Aperture ($2b$) of the single fracture is calculated (Maloszewski and Zuber, 1993) as

$$2b = QT_0/\pi r_L^2 = 0.534 \text{ mm}. \tag{3}$$

The matrix porosity corresponding to the calibrated A parameter is calculated as follows:

$$\phi_m = \left(A^2 b^2 / D_w\right)^{1/3} = 0.049, \tag{4}$$

where $D_w = 2.0 \times 10^{-9}$ m^2/s is used for iodide solution, and $D_m = \phi_m D_w$ ($n = 2$ in Equation 2) is assumed. The calculated porosity is reasonable in comparison with values obtained for matrix cores with a fracture-coating layer at the Finnsjon site (Skagius and Neretnieks, 1986). However, the calculated matrix porosity is much larger than that of intact matrix cores, indicating the presence of a degraded matrix zone with larger matrix porosity.

Based on the calculated fracture aperture and matrix porosity, and the calibrated A value, the effective matrix diffusion coefficient (D_m^e) is calculated as follows:

$$D_m^e = \left(Ab/\phi_m\right)^2 = 9.6 \times 10^{-11} \text{ m}^2/\text{s}. \tag{5}$$

The calculated D_m^e is reasonable compared to the laboratory values for cores with crushed materials and/or fracture-coating materials, whereas it is larger than that for intact matrix cores. In terms of the calculated matrix porosity and effective matrix diffusion coefficient, the

calibrated A value corresponds to that of the degraded matrix zone with fracture-coating materials.

3.3. Numerical Analysis (Calibration B)

To demonstrate the multi-process matrix diffusion occurring in this tracer test, numerical modeling was used with different values of D_m and ϕ_m for different diffusion zones. The study domain consists of a horizontal fracture (half aperture), an overlying degraded matrix zone, and an intact matrix zone. The domain is bounded by the fracture central plane at the bottom and by the central plane between two parallel fractures at the top, with the top and bottom boundaries impervious to both flow and transport. The entire domain consists of a fracture zone (0.267 mm, half aperture) and two matrix zones (1.00 m thick). The thickness of the degraded matrix zone was allowed to vary between 0 and 10 mm, on the basis of the measured thickness of fracture-coating materials (Skagius and Neretnieks, 1986). Since the flow field in the tracer test was convergent, a small wedge of $0.025\,\pi$ was used to represent the tracer transport system. Lateral boundaries in the vertical direction were assumed to be impervious. For flow simulation, a fixed discharge rate ($Q/160$) was specified at the wall of the pumping well, and a constant head was specified at the outer radial boundary at the injection well. For transport, a tracer mass of 0.9×10^{-5} moles/s was specified at the outer radial boundary, and an open boundary condition was specified at the pumping well. A fracture porosity of 1.0 was used, and no infilling material within the fracture was assumed. This assumption was based on a practical consideration that the effects of infilling materials could not be easily distinguished from those of a degraded zone. Therefore, the effects of a degraded zone to be discussed here for this tracer test also implicitly include the effects of infilling materials.

As discussed in Section 3.2, the calibrated three parameters in Calibration A represent the advection and dispersion effects in the fracture and the matrix-diffusion effect in the rock matrix. The fracture aperture (and hydraulic conductivity), calculated from the calibrated T_0 value, and the longitudinal dispersivity, calculated from the calibrated P_e value, were used directly in the numerical analysis. A matrix porosity of 0.3% and a matrix diffusion coefficient of 6×10^{-12} m^2/s were used for the intact zone. This D_m value was calculated internally using $D_m = \phi_m D_w$ with $D_w = 2.0 \times 10^{-9}$ m^2/s. For the degraded matrix zone, both its porosity and thickness varied to best match the measured breakthrough curve. The matrix porosity was allowed to vary between 0.05 and 0.15, and the matrix diffusion coefficient was calculated using $D_m = \phi_m D_w$. Therefore, in Calibration B, only two parameters (the thickness (b_1) and porosity) of the degraded matrix zone were calibrated.

The calibrated porosity and thickness of the degraded matrix zone are 10.0% and 4 mm, respectively. Specifically, the calibrated matrix diffusion coefficient for the degraded zone is 2.0×10^{-10} m^2/s. The measured matrix porosity and the average measured D_m value for a crushed zone with surface fracture-coating materials were 7.5% and 5.33×10^{-10} m^2/s, respectively. Therefore, the calibrated ϕ_m and D_m values are reasonable in comparison with their measured values from sample cores (Skagius and Neretnieks, 1986). The measured thickness of a layer of fracture-coating materials varied from 1 to 8 mm. Therefore, *the analysis of the multi-process model for the tracer test is consistent with the existence of a degraded matrix zone in terms of measured matrix porosity, matrix diffusion coefficient, and the thickness of fracture coating materials at the Finnsjon site.*

As shown in Figure 1, calibrated BTC matches the measured BTC well. The calibrated rising limb is identical to the measured one. The calibrated trend of slow increase in the middle platform is in good agreement with the measured one, although there are some fluctuations around the main trend in the measured BTC. The calibrated maximum tracer concentration (0.89 moles/m^3) at the 350th hr is close to the tracer concentration (0.9 moles/m^3) at the quasi-equilibrium status. At the quasi-equilibrium status, the measured concentration is identical to the concentration of injected tracer mass diluted by the pumped flow rate. The calibrated falling limb also closely matches the measured one. In comparison with the calibrated BTC in Calibration A (using the single-process matrix diffusion), the calibrated BTC in Calibration B is closer to the measured one at the later time of the middle platform. Specifically, the calibrated middle platform in Calibration B is higher than that in Calibration A, and the calibrated maximum tracer concentration is also higher than that (0.84 moles/m^3) in Calibration A. This is because the intact matrix zone in Calibration B plays an increasingly important role in the diffusion process at later time. Less tracer mass can be diffused into and stored in the matrix, because of the significantly smaller values for matrix porosity and matrix diffusion coefficient in the intact matrix zone than in the degraded zone. For the single-process model calibration, however, more tracer mass can be stored in the rock matrix, resulting in much longer time for the system to reach the quasi-equilibrium status. Therefore, *the multi-process model is more representative of the matrix diffusion processes involved in the tracer test than the single-process model.*

To further understand how the thickness and porosity of the degraded matrix zone affect tracer transport, a sensitivity analysis was conducted for two cases. In the first case, only the matrix porosity (and the matrix diffusion coefficient) of the degraded zone varied, with the thickness kept unchanged at 4 mm. As shown in Figure 2a, the shape of the tracer BTC is

sensitive to the matrix porosity of the degraded zone. The slope of the BTC in the middle platform increases with the matrix porosity, because a larger diffusion rate facilitates more tracer mass diffusing into the increasing void space. As a result, for a given time, the higher the matrix porosity and matrix diffusion coefficient of the degraded zone, the lower the tracer concentration. At the end of the constant-concentration-injection period, tracer concentration is similar for different porosity values, because a quasi-equilibrium condition has been reached and the same thickness of the degraded zone is used. This condition is controlled by the slow matrix diffusion process in the intact matrix zone after the tracer mass penetrates into the intact zone. The BTC's middle platform in this long-time constant-concentration-injection test is a very good indicator of high matrix porosity in the degraded zone. The matrix porosity also affects the rising and falling limbs. A larger porosity results in a more dispersed rising limb, because it allows for more tracer-mass storage at the early time of the test. Similarly, a larger porosity leads to a higher falling limb, because the more stored tracer mass in the degraded zone diffuses back to the fracture after the termination of tracer injection.

In the second case of the sensitivity analysis, only the thickness of the degraded zone varied, with the matrix porosity kept unchanged at 0.05. As shown in Figure 2b, the thickness of the degraded zone affects the time needed for reaching the equilibrium. For a smaller thickness, it takes less time to reach equilibrium, at which time the tracer concentration reaches its maximum value (0.9 moles/m^3). For a larger thickness (e.g., 10 mm), the equilibrium condition is not reached by the 350^{th} hour (the end of injection period), because more tracer mass can be stored in the degraded matrix zone. Thickness has little effect on the rising limb, because the diffusion rate (depending on the matrix diffusion coefficient and the concentration gradient at the fracture-matrix interface) is nearly independent of the thickness. However, the thickness has a

significant effect on the decay-like falling limb, because it takes time for the tracer mass (that has diffused into the degraded zone) to diffuse back into the fracture. Once the mass in the degraded zone is depleted, the back-diffusion process is dominated by the intact matrix zone.

In summary, the numerical analysis based on the developed multi-process matrix diffusion model is consistent with the measured porosity, diffusion coefficient, and thickness of the degraded zone with fracture-coating materials (Skagius and Neretnieks, 1986). The developed multi-process model is based on the field surveys, laboratory observations, and field tracer test analyses at the Finnsjon site as well as other fractured sites. The main objective of this technical note is to develop a new conceptual model based on physical transport processes observed, and to provide the evidence of the multi-process matrix diffusion from a unique field tracer test.

This tracer test was also used by the INTRACOIN project for international nuclide transport code intercomparison study (Davison et al., 1982; Swedish Nuclear Power Inspectorate, 1986), and analyzed by three research teams using different conceptual models. These models included the multi-channel model for field-scale dispersion with diffusion into the matrix, the stagnant water model, and the traditional single-process matrix diffusion model (Hodgkinson and Lever, 1983). In the stagnant water model, the diffusion into the stagnant water in the fracture was used to interpret a matrix diffusion coefficient much larger than the laboratory values obtained on intact rock cores. The diffusion into the rock matrix was also included in the stagnant water model. In the multi-channel model, several flow paths were assumed to exist, and the overall BTC was decomposed arbitrarily into contributing BTCs, which were obtained from the traditional single-process matrix diffusion model with advection and dispersion. When analyzing field tracer tests, one should first select the conceptual model consistent with the field

observations at the site of interest. The second concern is whether the transport parameters calibrated from field tracer tests can be extrapolated for predicting long-term, large-scale transport behavior (McKenna and Selroos, 2004).

3.4. Short- and Long-Term Effects

As shown in the above calibrations, the multi-process matrix diffusion model tracks all the diffusion processes in both the degraded and intact matrix zones shown in the field test, whereas the single-process model tracks only the dominant diffusion process within the degraded matrix zone, which is the case for many short-term field tracer tests.

To demonstrate the difference in the short-term and long-term transport behavior predicted by the two different models, we simulated tracer transport in a linear flow field with pore velocity of 0.2 m/d. On the basis of the numerical model in Calibration B, the following changes were undertaken for the transport simulations: (1) the domain was changed to a cube (1,000 m long along the single fracture, 1.000267 thick, and 2 m wide); (2) a uniform discretization of 2 m was used along the fracture; (3) a tracer solution of 80.7 g/L was injected for the first 0.01 day only. For comparison, three cases were defined: in Case A, the calibrated (field-scale) matrix diffusion coefficient ($D_m = 0.96 \times 10^{-10}$ m^2/s) and the porosity ($\phi_m = 0.049$) in Calibration A (for the single-process model) were used for the entire rock matrix. In Case B, the calibrated matrix porosity and matrix diffusion coefficient ($\phi_m = 0.1$ and $D_m = 2 \times 10^{-10}$ m^2/s) in Calibration B were used for the 4 mm thick degraded zone, and the lab-scale values ($\phi_m = 0.003$ and $D_m = \phi_m D_w = 6 \times 10^{-12}$ m^2/s) were used for the intact matrix zone. In Case C, the lab-scale matrix porosity and matrix diffusion coefficient for intact matrix rock was used for the entire rock matrix.

Figure 3 shows the simulated breakthrough curves for the three cases at 10, 100, and 1,000 m from the source point. At the smallest scale (10 m), the multi-process model produces a higher but later concentration peak than the single-process model. The later peak in Case B may be caused by the higher porosity and diffusion coefficient values of the degraded zone in Case B than in Case A. The higher peak in Case B may result from a smaller diffusion coefficient and porosity in the intact matrix zone. There is a relatively flat plateau where the concentration changes slowly with time in the double-logarithm scale. The plateau in Case B is lower than that in Case A, because less tracer mass has been stored in the rock matrix. At the later time, Case B produces a longer tail than Case A. At the middle scale (100 m), the BTC in Case B is very different from that in Case A, in that a peak with a plateau occurs in Case B, whereas a single peak without the plateau occurs in Case A. At the largest scale (1,000 m), the multi-process model produces much earlier breakthrough, a longer breakthrough time period, and a lower and flatter concentration peak than the single-process model. The huge differences in the breakthrough curves between the two models are attributed to the existence of the intact matrix zone in Case B. Therefore, at different scales, *different tracer-transport behavior is obtained using the different transport models.*

In contrary, Case B produces breakthrough curves similar to those in Case C at the three observation scales. In particular, the two cases produce very similar tails at the later time, which is believed to be a function of the intact zone, with low matrix porosity and matrix diffusion coefficient. This is because the majority (93.7%) of matrix pore space in the intact matrix zone is the same for both cases. The only difference is that the tracer in Case B breaks through later than in Case C, and the delayed breakthrough in Case B is attributed to the larger matrix porosity and matrix diffusion coefficient of the degraded matrix zone.

4. Conclusions

Here, we propose a conceptual model of multi-process matrix diffusion, based on the enhanced matrix diffusion (involving single fractures) observed at a number of tracer test sites and laboratory observations of a degraded matrix zone. The sequence of multiple diffusion processes with different matrix-diffusion-coefficient values consists of (1) diffusion into stagnant water and infilling materials in fractures, (2) diffusion into a degraded matrix zone adjacent to fractures, and (3) further diffusion into an intact matrix zone away from fractures. The accuracy of the multi-process matrix diffusion model was confirmed by a unique field tracer test (Gustafsson and Klockars, 1981) conducted using long-time constant-concentration injection. Analysis of the tracer test, based on numerical modeling of multi-process matrix diffusion, has been used to support our conceptual model. The excellent match between calibrated and measured breakthrough curves indicates that the diffusion process into the degraded matrix zone controls the steep rising limb and the decay-like falling limb of the measured breakthrough curve. Similarly, the diffusion process into the intact matrix zone controls the later portion of the middle platform of the breakthrough curve. Finally, the transition from the former to the latter process controls the middle platform, which features a slowly increasing tracer concentration before the equilibrium condition is reached.

The multi-process matrix diffusion model was compared with the traditional single-process model for analyzing the tracer test and for predicting tracer transport behavior at different scales in a linear flow field. The analysis comparison indicates that matrix porosity and matrix diffusion coefficient values higher than those of the intact matrix zone are needed to match the measured breakthrough curve in both models. However, the prediction comparison demonstrates that the multi-process model produces breakthrough curves significantly different from those obtained by the single-process model, and the difference becomes larger at a larger

scale. The significant difference indicates that distinguishing matrix diffusion processes within different matrix zones is critical to prediction of large-scale tracer transport behavior in the field.

References

Andersson, P., Byegård, J., Tullborg, E., Doe, T., Hermanson J. and Winberg, A.: 2004, In situ tracer tests to determine retention properties of a block scale fracture network in granitic rock at the Äspö Hard Rock Laboratory, Sweden, *J. Contam. Hydrol.*, **70** (3-4), 271-297.

Boving, T. B. and Grathwohl, P.: 2001, Tracer diffusion coefficients in sedimentary rocks: Correlation to porosity and hydraulic conductivity, *J. Contam. Hydrol.*, **53**, 85–100.

Davison, C., Goblet, P. and Neretnieks, I.: 1982, Tracer tests in fissured rock for model testing in INTRACOIN; Appendix 1, introductory description of tracer tests at Finnsjon and summary of important data.

Gustafsson, E. and Klockars, C. E.: 1981, Studies on groundwater transport in fractured crystalline rock under controlled conditions using non-radioactive tracers, KBS TR-81-07, Nuclear Fuel Safety Project, Stockholm, Sweden.

Hodgkinson, D. P. and Lever, D. A.: 1983, Interpretation of a field experiment on the transport of sorbed and non-sorbed tracers through a fracture in crystalline rock, *Radioact. Waste Manag. Nucl. Fuel. Cycle*, **4** (2), 129–158.

Liu, H. H., Salve, R., Wang, J. S., Bodvarsson, G. S. and Hudson, D.: 2004, Field investigation into unsaturated flow and transport in a fault: model analyses, *J. Contam. Hydrol.*, **74**, 39–59.

Maloszewski, P. and Zuber, A.: 1993, Tracer experiments in fractured rocks: Matrix diffusion and the validity of models, *Water Resour. Res.*, **29**(8), 2723-2735.

Maloszewski, P., Herrmann, A. and Zuber, A.: 1999, Interpretation of tracer tests performed in a fractured rock of the Lange Bramke Basin, Germany, *Hydrogeol. J.*, **7**, 209–218.

McKenna, S. A. and Selroos, J.-O.: 2004, Constraining performance assessment models with tracer test results: a comparison between two conceptual models, *Hydrogeol. J.*, **12**, 243–256.

Neretnieks, I.: 2002, A stochastic multi-channel model for solute transport—analysis of tracer tests in fractured rock, *J. Contam. Hydrol.*, **55**, 175–211.

Polak, A., Grader, A. S., Wallach, R. and Nativ, R.: 2003, Chemical diffusion between a fracture and the surrounding matrix: Measurement by computed tomography and modeling, *Water Resour. Res.*, **39**(4), 1106, doi:10.1029/2001WR000813.

Reimus, P., Pohll, G., Mihevc, T., Chapman, J., Haga, M., Lyles, B., Kosinski, S., Niswonger, R. and Sanders P.: 2003, Testing and parameterizing a conceptual model for solute transport in a fractured granite using multiple tracers in a forced-gradient test, *Water Resour. Res.*, **39**(12), 1356, doi:10.1029/2002WR001597.

Skagius, K. and Neretnieks, I.: 1986, Porosities and diffusivities of some nonsorbing species in crystalline rocks, *Water Resour. Res.*, **22**(3), 389–398.

Swedish Nuclear Power Inspectorate: 1986, Final report levels 2 and 3, model validation and uncertainty analysis, INTRACOIN, International Nuclide Transport Code Intercomparison Study, Stockholm, Sweden.

Tokunaga, T. K. and Wan, J.: 2001, Surface-zone flow along unsaturated rock fractures, *Water Resour. Res.*, **37**(2), 287–296.

Wealthall, G. P., Steele, A., Bloomfield, J. P., Moss, R. H. and Lerner, D. N.: 2001, Sediment filled fractures in the Permo-Triassic sandstones of the Cheshire Basin: observations and implications for pollutant transport, *J. Contam. Hydrol.*, **50**, 41–51.

Weisbrod, N., Dahan, O. and Adar, E. M.: 2002, Particle transport in unsaturated fractured chalk under arid conditions, *J. Contam. Hydrol.*, **56**, 117–136.

Wu, Y. S., Liu, H. H. and Bodvarsson, G. S.: 2004, A triple-continuum approach for modeling flow and transport processes in fractured rock, *J. Contam. Hydrol.*, **73**, 145-179.

Zhou, Q., Liu, H. H., Bodvarsson, G. S. and Oldenburg C. M.: 2003, Flow and transport in unsaturated fractured rock: effects of multiscale heterogeneity of hydrogeologic properties, *J. Contam. Hydrol.*, **60**, 1-30.

Zhou, Q., Liu, H. H., Molz, F. J., Zhang, Y., and Bodvarsson, G. S.: 2005, Field-scale effective matrix diffusion coefficient for fractured rock: Results from literature survey, *Water Resour. Res.* (in review).

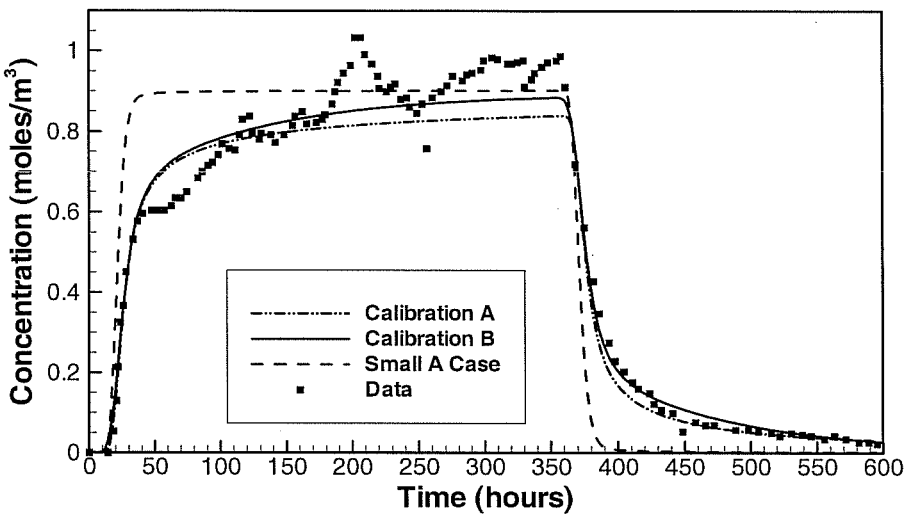

Figure 1. Matches between measured breakthrough curve and calibrated breakthrough curves using (1) a semi-analytical solution with single-process matrix diffusion (Calibration A), (2) a numerical analysis with multi-process matrix diffusion (Calibration B), and (3) a case with a small porosity and matrix diffusion coefficient of the intact matrix zone

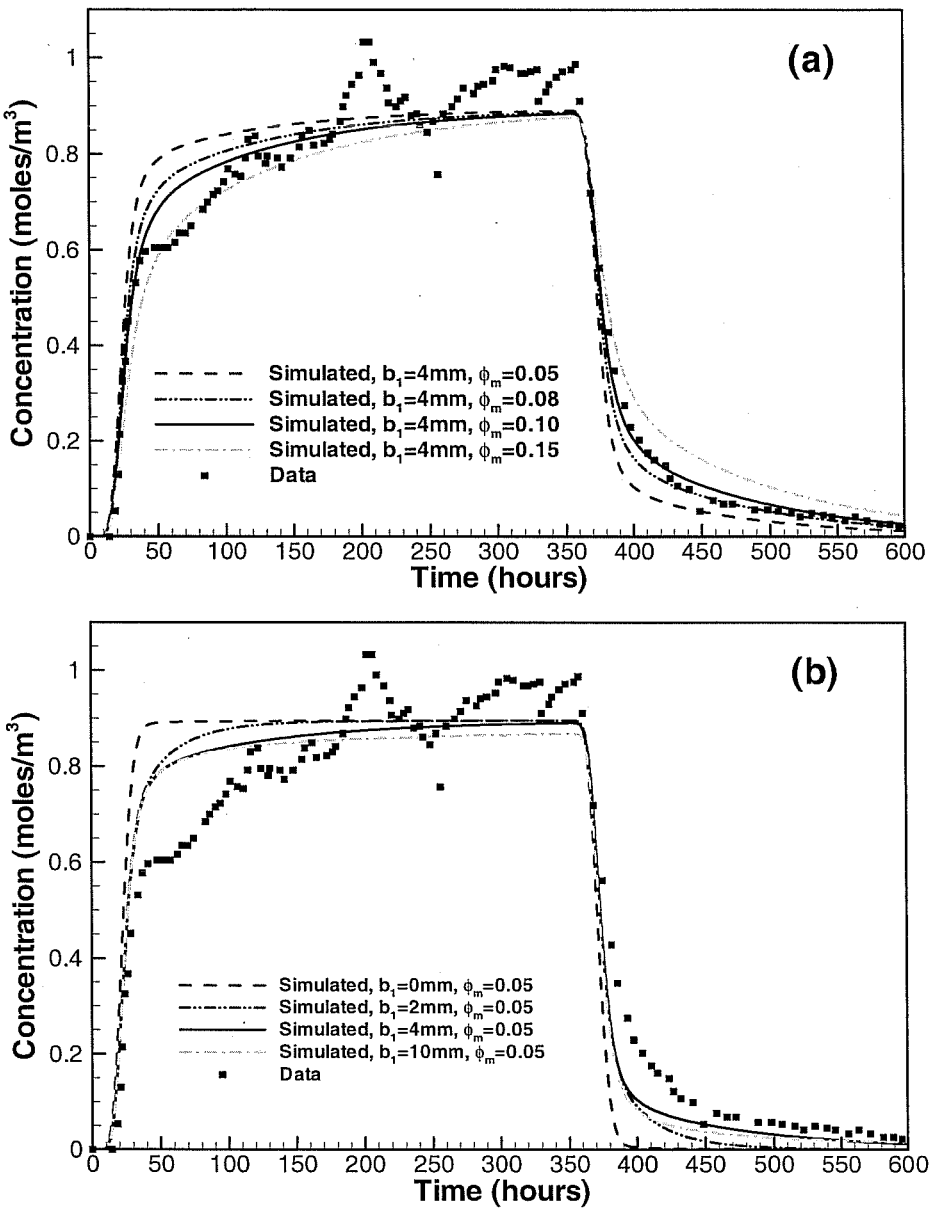

Figure 2. Sensitivity analysis of the tracer breakthrough curve to (a) the porosity (ϕ_m) and (b) the thickness (b_1) of the degraded matrix zone

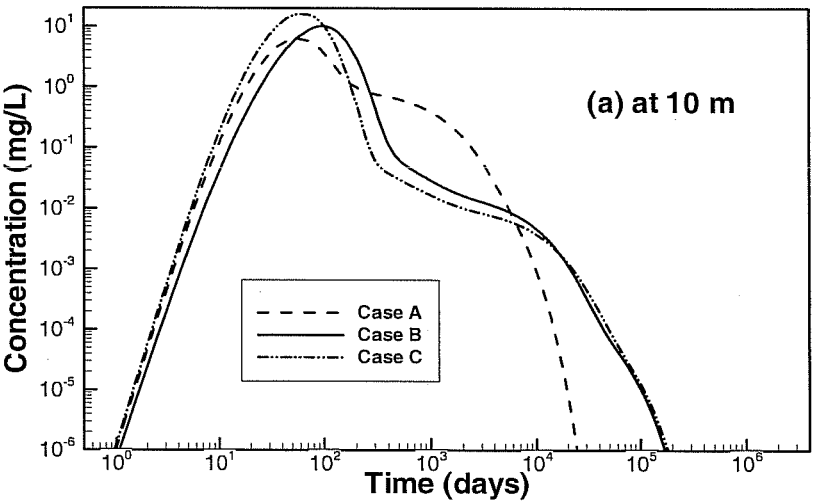
(a) at 10 m
Case A
Case B
Case C
Concentration (mg/L)
Time (days)

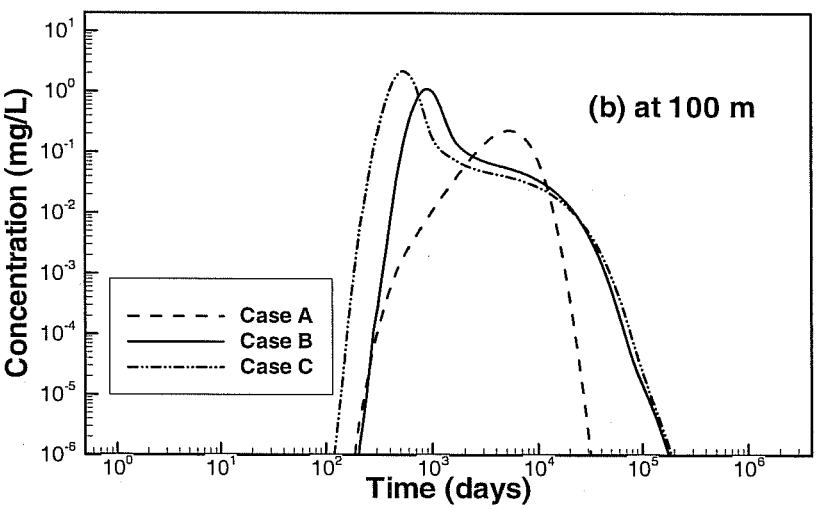
(b) at 100 m
Case A
Case B
Case C
Concentration (mg/L)
Time (days)

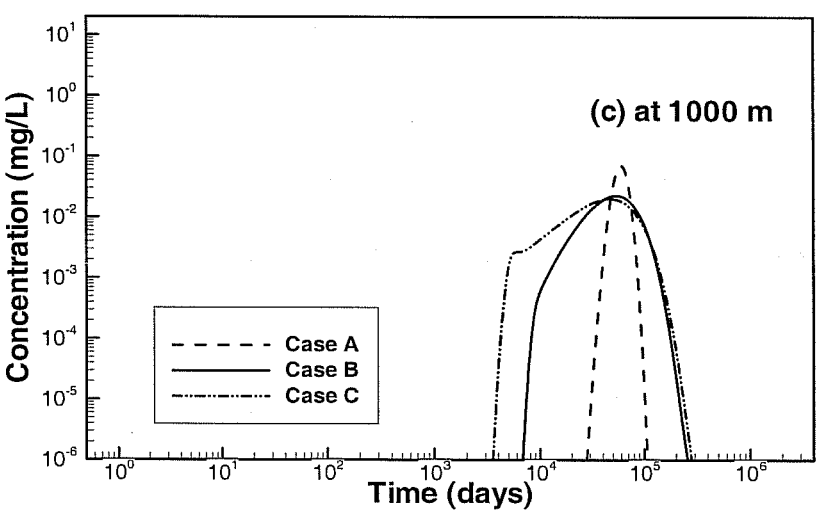
(c) at 1000 m
Case A
Case B
Case C
Concentration (mg/L)
Time (days)

Figure 3. Predicted breakthrough curves for Case A (calibrated matrix diffusion coefficient and porosity in Calibration A using the single-process model), Case B (calibrated parameters in Calibration B using the multi-process model), and Case C (measured lab-scale parameters for the intact matrix zone) at (a) 10 m, (b) 100 m, and (c) 1,000 m